

Open-Vocabulary Animal Keypoint Detection with Semantic-feature Matching

Hao Zhang · Lumin Xu · Shenqi Lai · Wenqi Shao · Nanning Zheng · Ping Luo ·
 Yu Qiao · Kaipeng Zhang*

Received: date / Accepted: date

Abstract Current image-based keypoint detection methods for animal (including human) bodies and faces are generally divided into full-supervised and few-shot class-agnostic approaches. The former typically relies on laborious and time-consuming manual annotations, posing considerable challenges in expanding keypoint detection to a broader range of keypoint categories and animal species. The latter, though less dependent on extensive manual input, still requires necessary support images with annotation for reference during testing. To realize zero-shot keypoint detection without any prior annotation, we introduce the **Open-Vocabulary Keypoint Detection (OVKD)** task, which is innovatively designed to use text prompts for identifying arbitrary keypoints across any species. In pursuit of this goal, we have developed a novel framework named **Open-Vocabulary Keypoint Detection with Semantic-feature Matching (KDSM)**. This framework synergistically combines vision and language models, creating

an interplay between language features and local keypoint visual features. KDSM enhances its capabilities by integrating **Domain Distribution Matrix Matching (DDMM)** and other special modules, such as the **Vision-Keypoint Relational Awareness (VKRA)** module, improving the framework's generalizability and overall performance. Our comprehensive experiments demonstrate that KDSM significantly outperforms the baseline in terms of performance and achieves remarkable success in the OVKD task. Impressively, our method, operating in a zero-shot fashion, still yields results comparable to state-of-the-art few-shot species class-agnostic keypoint detection methods. We will make the source code publicly accessible.

Keywords Open vocabulary · Open set · Keypoint Detection · Pose estimation

1 Introduction

Animal keypoint detection, a fundamental and important task in computer vision, is dedicated to accurately identifying and localizing animals' keypoints within images. This task is crucial in the detailed study and analysis of animal (including human) bodies and faces. The accurate location of these keypoints plays a vital role in various applications, ranging from in-depth behavioral studies to automated monitoring systems.

Traditional keypoint detection methods (Tu et al., 2023; Xu et al., 2022b; Zhang et al., 2023) have largely depended on labor-intensive, time-consuming manual annotations under full supervision. This heavy reliance creates significant and challenging barriers when expanding keypoint detection to encompass new keypoint categories and animal species. Advanced few-shot species class-agnostic keypoint detection methods, as extensively detailed in studies like (Shi et al., 2023; Xu et al., 2022a), represent progress in reducing the

* Corresponding Author

Hao Zhang · Nanning Zheng
 Institute of Artificial Intelligence and Robotics, Xi'an Jiaotong University, Xi'an, China
 E-mail: zhanghao520@stu.xjtu.edu.cn, nnzheng@mail.xjtu.edu.cn

Kaipeng Zhang · Wenqi Shao · Yu Qiao
 Shanghai AI Laboratory, Shanghai, China
 E-mail: zhangkaipeng@pjlab.org.cn, shaowenqi@pjlab.orn.cn, qiaoyu@pjlab.org.cn

Lumin Xu
 The Chinese University of Hong Kong, Hong Kong, China
 E-mail: luminxu@link.cuhk.edu.hk

Shenqi Lai
 Zhejiang University, Hangzhou, China
 E-mail: laishenqi@fabu.ai

Ping Luo
 The University of Hong Kong, Hong Kong, China
 E-mail: pluo@cs.hku.edu

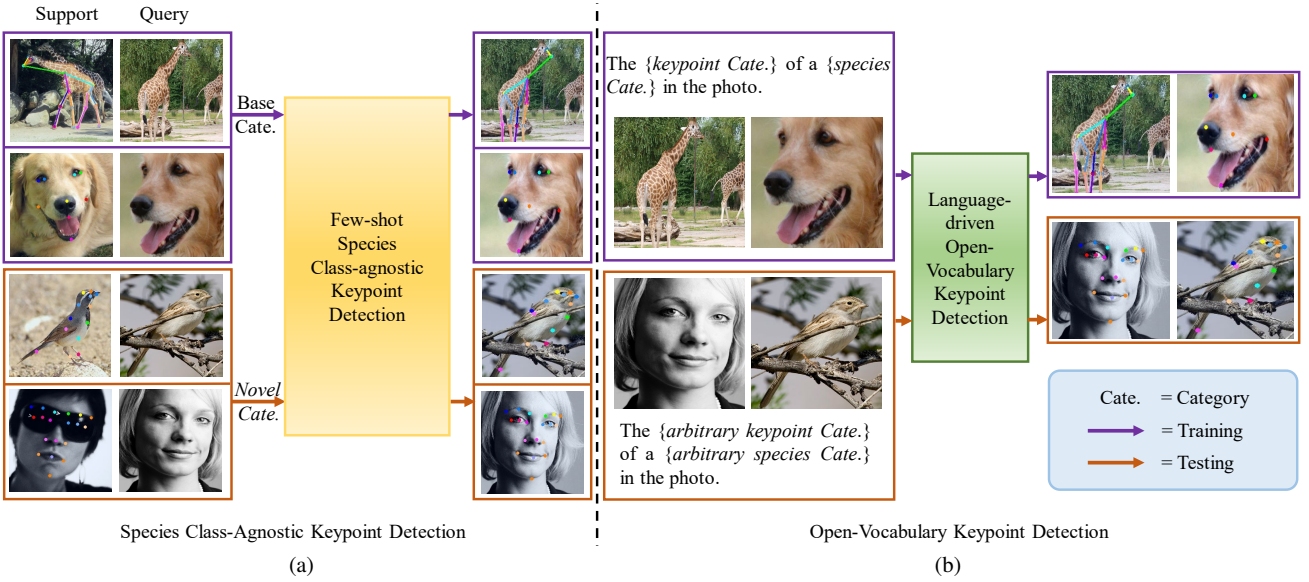


Fig. 1: Few-shot Species Class-Agnostic Keypoint Detection vs. Language-driven Open-Vocabulary Keypoint Detection. (a) Current few-shot species class-agnostic keypoint detection needs support images for guidance during training and testing to detect keypoints in new species. (b) Language-driven OVKD aims to use text prompts that embed both *{animal species}* and *{keypoint category}* as semantic guidance to localize arbitrary keypoints of any species.

reliance on extensive manual annotations to adapt new keypoint categories and animal species. As illustrated in Fig. 1 (a), these methods necessitate a small number of annotated support images for keypoint references during testing. In this paper, we further accomplish a more challenging task, which detects arbitrary keypoint in a zero-shot fashion without prior annotation during testing.

The potential of Vision-language models (VLMs) (Jia et al., 2021; Radford et al., 2021) inspires our approach. VLMs have shown success in joint modeling of visual and text information, contributing to their exceptional zero-shot learning ability in various tasks, including object detection, semantic segmentation, video classification, and others (Weng et al., 2023; Xu et al., 2023; Yao et al., 2022). However, there is a lack of research specifically addressing keypoint detection methods within this context. Motivated by VLM advancements, we introduce the language-driven **Open-Vocabulary Keypoint Detection** (OVKD) task (hereafter referred to as OVKD). Specifically, OVKD is designed to identify a broad spectrum of *(animal species, keypoint category)* pairs, including those not encompassed in the original training dataset. As shown in Fig. 1 (b), OVKD uses the image and text description of the keypoints to realize keypoint detection.

Building upon this concept, our initial strategy involves adopting a baseline framework (see Fig. 2) that utilizes language models to obtain text embeddings for the descriptions of *(animal species, keypoint category)* pairs. Then the baseline integrates the text embeddings with visual features using matrix multiplication and generates keypoint heatmaps. How-

ever, the limitation of this simple feature aggregation becomes evident in its lack of effective interaction between text and local visual features, hindering its ability to comprehend the local features of images and accurately localize specific keypoints. To address this, we emphasize the need for deeper interaction between text and local visual features of the image.

To overcome the limitations of the baseline framework in OVKD, we develop an advanced framework named **Open-Vocabulary Keypoint Detection with Semantic-feature Matching** (KDSM). KDSM introduces a **Domain Distribution Matrix Matching** (DDMM) technique and incorporates other special modules, such as a **Vision-Keypoint Relational Awareness** (VKRA) module, a keypoint encoder, a keypoint adapter, a vision head, and a vision adapter, among others. The VKRA module uses attention blocks to enhance the interaction between text embeddings and local keypoint features. This facilitates a deeper exploration and understanding of the complex relationships between various local keypoint locations and text prompts during training. Considering that the combinations of *(animal species, keypoint category)* pairs are virtually infinite, it becomes impractical to construct a heatmap channel for every pair like full-supervised and few-shot species class-agnostic keypoint detection methods. Therefore, we propose DDMM, which utilizes clustering techniques to group the text features of different descriptions of *(animal species, keypoint category)* pairs. It allows semantically similar combinations to share a heatmap channel representation. After grouping, the matching loss between text and heatmap features can be used to further align text features

and keypoint visual features. During testing, DDMM can also assign new text descriptions to specific groups, enabling the capability of zero-shot keypoint detection.

We conduct extensive experiments to evaluate the efficacy of our proposed method. The results emphatically demonstrate that our KDSM framework excels in OVKD, significantly surpassing the performance of the baseline framework. Notably, KDSM exhibits impressive zero-shot capabilities and comparable performance to the state-of-the-art few-shot species class-agnostic keypoint detection methods. The primary contributions of our research are summarized as follows:

- We introduce the task of **Open-Vocabulary Keypoint Detection** (OVKD), designed to utilize text prompts for detecting a diverse range of keypoint categories across different animal species in a zero-shot fashion.
- We introduce **Keypoint Detection with Semantic-feature Matching** (KDSM), a highly effective framework for achieving OVKD. It leverages the strengths of advanced language models, particularly by proposing the DDMM technique and integrating it with other special modules, such as the VKRA module, to significantly enhance the performance of OVKD.
- Extensive experimental results demonstrate the effectiveness of KDSM, achieving remarkable performance in OVKD and outperforming the baseline framework by a large margin. Furthermore, though KDSM performs in a zero-shot fashion, it achieves results comparable to state-of-the-art few-shot species class-agnostic keypoint detection methods.

2 Related Works

Traditionally, the main research direction in keypoint detection has been full-supervised methods. This approach concentrated on improving keypoint detection accuracy via advancements in neural network architectures (Tu et al., 2023; Wang et al., 2020; Xu et al., 2022b; Zhang et al., 2023) and the development of new species datasets (Brown et al., 2020; Labuguen et al., 2021). However, these methods are confined to specific species or keypoint categories, limiting their adaptability to new types. Emerging few-shot category-agnostic keypoint detection techniques have started to address this, reducing the need for extensive annotations for novel species with a small number of annotated support images. We take this a step further by removing the necessity for image labeling and using language models to detect keypoints in a zero-fashion, Open-Vocabulary approach. In Section 2.1, we’ll review the few-shot category-agnostic keypoint detection methods, and in Section 2.2, we’ll present related works in Open-Vocabulary learning.

2.1 Advancements in Few-shot Species Class-agnostic Keypoint Detection

A significant advancement in keypoint detection is the advent of few-shot species class-agnostic techniques (Xu et al., 2022a), which can identify keypoints across various animal species without category-specific training. However, these techniques commonly rely on “support images” during the training and testing phases. This reliance, characteristic of methods like MAML (Finn et al., 2017), Fine-tune (Nakamura and Harada, 2019), FS-ULUS (Lu and Koniusz, 2022), POMNet (Xu et al., 2022a), and CapeFormer (Shi et al., 2023), limits their applicability to new species or keypoints.

Specifically, POMNet (Xu et al., 2022a) initially proposed the few-shot species class-agnostic keypoint detection task and created the MP-100 expert dataset for it. CapeFormer (Shi et al., 2023) presents a two-stage framework incorporating techniques like a query-support refine encoder and a similarity-aware proposal generator for category-agnostic detection, shifting focus from heatmap prediction to keypoint position regression. In contrast, our **Open-Vocabulary Keypoint Detection** (OVKD) task moves away from reliance on support images. OVKD leverages text prompts containing both $\{\text{animal species}\}$ and $\{\text{keypoint category}\}$, offering semantic guidance for detecting any keypoint in any species. This novel approach is aligned with zero-shot learning principles and marks a stride towards open-world animal body and facial keypoint detection.

2.2 Exploring Open-Vocabulary Learning in Computer Vision

Open-Vocabulary learning, a burgeoning field in computer vision, has been explored in various tasks, including object detection (Bangalath et al., 2022; Yao et al., 2022), semantic segmentation (Li et al., 2022; Xu et al., 2023), 3D object recognition (Weng et al., 2023; Zhu et al., 2023) and video classification (Ni et al., 2022; Qian et al., 2022). The advent of vision-language models like CLIP (Radford et al., 2021) and ALIGN (Jia et al., 2021) has underscored their potential in tasks that require simultaneous processing of visual and text data, ideal for open-world learning scenarios.

While existing research in Open-Vocabulary learning excels in image-level classification (Zhu et al., 2023), per-pixel classification (Li et al., 2022), and mask classification (Xu et al., 2023), keypoint detection poses a unique challenge. It demands not only a global understanding of the image but also precise localization of specific keypoints within it. To tackle this, we propose a novel technique called “Domain Distribution Matrix Matching.” This technique transforms keypoint detection into a task of aligning semantic feature distributions from input text prompts with the detected heatmaps,

thereby enhancing the accuracy and efficiency of the detection process.

3 Method

In this section, we begin by defining the **Open-Vocabulary Keypoint Detection** (OVKD) task in Section 3.1. We then present a baseline framework in Section 3.2, which offers a straightforward solution to the task. In Section 3.3, we introduce our proposed Open-Vocabulary Keypoint Detection with Semantic-feature Matching (KDSM) framework, outlining its unique design and capability.

3.1 Problem Formulation: Open-Vocabulary Keypoint Detection

We introduce a novel task termed **Open-Vocabulary Keypoint Detection** (OVKD) for animal (including human) body and face keypoint localization. The goal of OVKD is to develop a framework capable of detecting arbitrary keypoints in images, even if the animal species or keypoint category is not present in the training data. The advancements in vision-language models such as CLIP (Radford et al., 2021), allow the keypoint detectors to take advantage of powerful language models to achieve language-driven OVKD (unless otherwise specified, OVKD always refers to language-driven OVKD).

For the language-driven OVKD, text prompts are leveraged to guide the framework in understanding the semantic information and locating specific keypoints. Assuming we have a training set \mathcal{D}_{train} and a test set \mathcal{D}_{test} , $\mathcal{D}_{train} = \{(\mathbf{I}, T(s_i, k_j)_{j=1}^{\mathbb{K}_{s_i}})\}_{i=1}^{\mathbb{S}}$, $\mathcal{D}_{test} = \{(\mathbf{I}, T(s'_i, k'_j)_{j=1}^{\mathbb{K}'_{s'_i}})\}_{i=1}^{\mathbb{S}'}$. Here, \mathbf{I} represents images, and $T(s_i, k_j)$ denotes the text prompts constructed based on species s_i and keypoint category k_j . \mathbb{S} and \mathbb{K}_{s_i} represent the number of species and the number of keypoint categories of species s_i in the training set, respectively, while \mathbb{S}' and $\mathbb{K}'_{s'_i}$ represent the number of species and the number of keypoint categories of species s'_i in the test set, respectively. The test set includes *(animal species, keypoint category)* pairs not covered in the training dataset, requiring the detector to identify arbitrary keypoints as per the text prompts.

3.2 Baseline: A Simple Framework for OVKD

In order to tackle the challenging **Open-Vocabulary Keypoint Detection** (OVKD) task, we build a baseline framework that is able to predict arbitrary keypoint category of any animal species as shown in Fig. 2. The baseline method constructs text prompts for the OVKD task and extracts text embedding using a Text_Encoder. The Vision_Encoder is applied to extract visual features of the input image simultaneously. Then, the

visual and text features are integrated by matrix multiplication to output heatmaps of keypoints defined by text prompts.

Text Prompts Construction. In this step, we utilize the template “The *{keypoint category}* of a *{animal species}* in the photo.” to assist language models in effectively grasping the task. For example, if “giraffe body” is the animal species and “neck” the keypoint category, the prompt becomes: “The neck of a giraffe body in the photo.” This consistent template is applied across various animals and keypoints, with placeholders adjusted accordingly. Utilizing this template enables the language model to concentrate on the interplay between animal species and keypoints, facilitating smooth generalization to new species and keypoints within the Open-Vocabulary framework.

Text Feature Extraction. Employing the pre-trained CLIP Text_Encoder (Radford et al., 2021), we process the preprocessed text prompts $T = \{T_1, T_2, \dots, T_K\}$ for an image with K text prompts:

$$\mathbf{T} = \text{Keypoint_Adapter}(\text{Text_Encoder}(T)), \quad (1)$$

where $\text{Text_Encoder}(T) \in \mathbb{R}^{K \times C_0}$ represents the extracted text features. Keypoint_Adapter is a two-layer Multi-layer Perceptron (MLP) used to refine these features and make them compatible with the image feature representations. This refinement produces a semantic feature space $\mathbf{T} \in \mathbb{R}^{K \times C}$ (with $K = 100, C = 64$ in our setup). Given the varying numbers of keypoints across different species, we fill in $K - k$ fixed placeholder text features. The text features are extracted from the prompt “There is not the keypoint we are looking for.”

Vision Feature Extraction. Given an input image I , we train a Vision_Encoder and a Vision_Head to extract image features:

$$\mathbf{V} = \text{Vision_Head}(\text{Vision_Encoder}(I)), \quad (2)$$

where $\mathbf{V} \in \mathbb{R}^{C \times H \times W}$ ($H = 64, W = 64$ in our implementation) represents vision feature. We utilize pre-trained models, such as ResNet (He et al., 2016) and ViT (Dosovitskiy et al., 2020), as the backbone of the Vision_Encoder. These models are known to be effective in extracting hierarchical visual features from images. The Vision_Head, inspired by SimpleBaseline (Xiao et al., 2018), is composed of three deconvolutional layers. These layers serve to upsample the low-resolution feature maps acquired from the image encoder, thereby successfully recovering spatial information and enabling accurate keypoint localization.

Keypoint Heatmap Prediction. The objective of this framework is to predict keypoint localization by aggregating semantic text and spatial visual features. To calculate the similarity between the text feature and pixel-level visual representation, the extracted features are combined through matrix multiplication:

$$\mathbf{H} = \mathbf{T} \times \mathbf{V}, \quad (3)$$

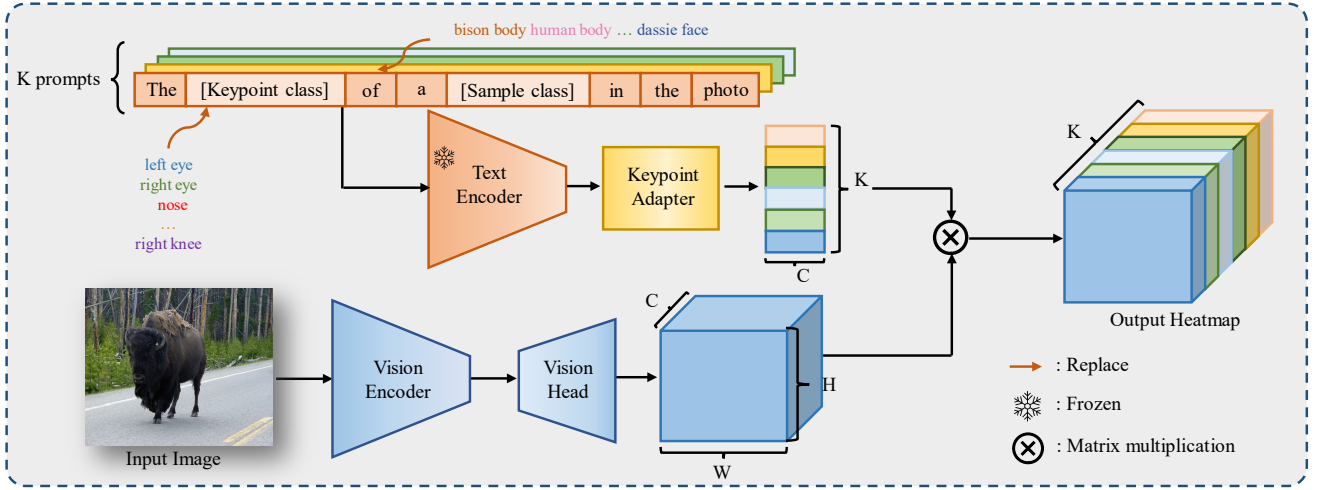


Fig. 2: An overview of the baseline method for OVKD. The baseline comprises a Vision_Encoder, a Text_Encoder, a Vision_Head and a Keypoint_Adapter. The Keypoint_Adapter is applied to optimize the relevance of text features with the image features and produce the text feature with the shape of $C \times K$, where C and K represent the number of channel and text prompts, respectively. The Vision_Head produces the visual feature with the shape of $C \times H \times W$, where H and W represent the height and width, respectively.

where $\mathbf{H} \in \mathbb{R}^{K \times H \times W}$ denotes predicted heatmaps. And the framework supports multiple text prompt inputs for detecting several keypoints simultaneously. The model training is supervised using Mean Squared Error (MSE) loss between these predicted heatmaps \mathbf{H} and the ground truth heatmaps $\mathbf{G} \in \mathbb{R}^{K \times H \times W}$. During training, the Text_Encoder remains frozen, while other parameters are trainable. The matrix multiplication operation conducts a transformation of visual features to the output heatmap spaces, driven by the semantic information contained in the text prompts.

3.3 Open-Vocabulary Keypoint Detection with Semantic-feature Matching

In this section, we propose a novel framework, namely **Open-Vocabulary Keypoint Detection with Semantic-feature Matching (KDSM)**, to address the limitations of the baseline OVKD framework. The baseline framework just uses simple feature aggregation, which fails to effectively capture the intricate relationship between text and local visual features and establish clear connections between them, leading to less than optimal keypoint detection. Therefore, KDSM proposes **Domain Distribution Matrix Matching (DDMM)** and adopts some special modules to address the above problems, such as a **Vision-Keypoint Relational Awareness (VKRA)** module, a keypoint encoder, a keypoint adapter, a vision head, and a vision adapter, among others.

As depicted in Fig. 3, KDSM initially constructs text prompts and extracts text features similarly to the baseline approach. However, it then employs the VKRA module to fa-

cilitate a deeper exploration and understanding of the complex relationships between various local keypoint locations and text prompts during training. Finally, DDMM is proposed to capture cross-species keypoint-level relationships to further enhance the generalization ability of KDSM. Notably, KDSM supports multiple text prompt inputs for detecting several keypoints simultaneously.

Vision-Keypoint Relational Awareness Module. Within our framework, the vision-keypoint relational awareness module, incorporating a series of Transformer blocks inspired by (Pan et al., 2020), is an essential design. It comprises two main components: Self-Attention (Vaswani et al., 2017) (Self_Attn.) and Cross-Attention (Carion et al., 2020) (Cross_Attn.). The self-attention layers are designed to enhance the interaction among text embeddings of the given sample. They amalgamate keypoint features as follows:

$$\mathbf{Y}_t = \text{Self_Attn.}(\text{Text_Encoder}(\mathbf{T})). \quad (4)$$

The refined keypoint features \mathbf{Y}_t elucidate the relationships of text semantic concepts among the keypoints of a specific species.

The cross-attention layers use the output features from the Vision_Encoder as the query, while the refined features \mathbf{Y}_t serve as the key and value. This mechanism facilitates interaction between the context-aware visual features Vision_Encoder(I) and the refined features \mathbf{Y}_t to enhance the vision representation:

$$\tilde{\mathbf{V}} = \text{Cross_Attn.}(\text{Vision_Encoder}(I), \mathbf{Y}_t) \quad (5)$$

The updated visual features $\tilde{\mathbf{V}}$ effectively capture the relationships between local visual features and keypoint text

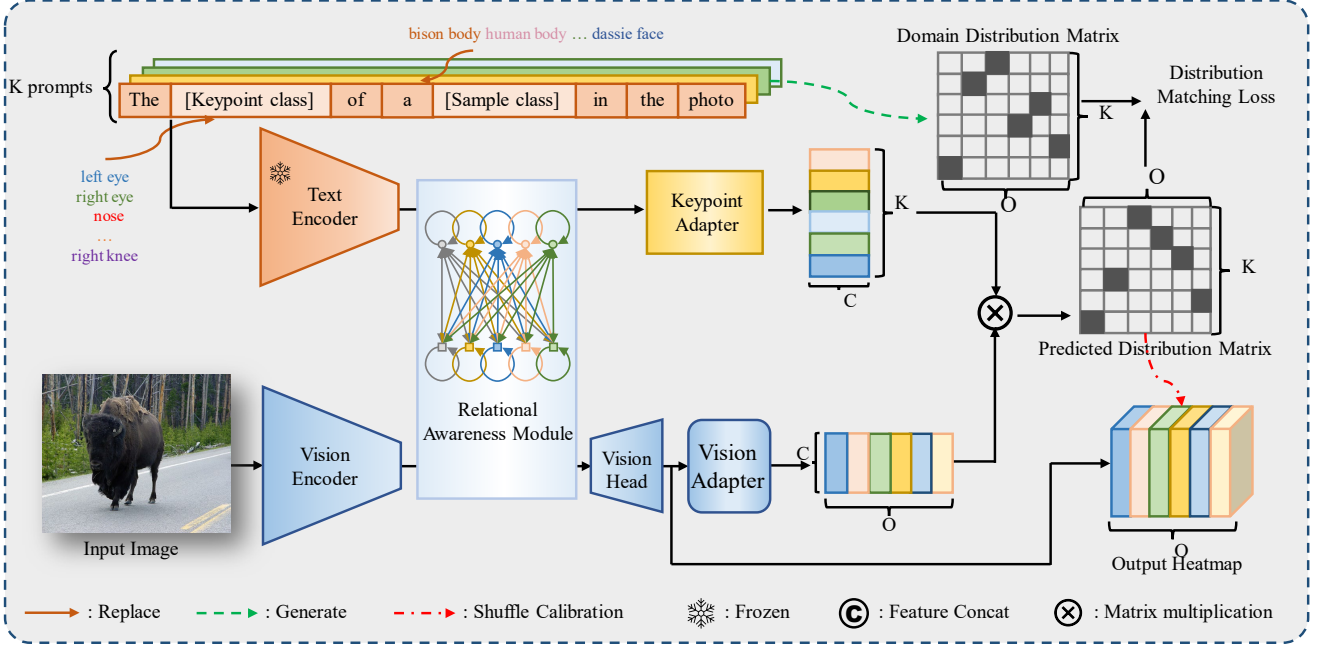


Fig. 3: An overview of KDSM. KDSM comprises a Vision_Encoder, a Text_Encoder, a Keypoint_Adapter, a Vision_Adapter and a Vision_Head similar to the baseline. The vision-keypoint relational awareness module adjusts visual features according to their associations with keypoints. The Vision_Adapter is employed to modify the feature shape so that it matches the text features' shape. Similarity is calculated between the adjusted features and text semantic features, resulting in a predicted distribution matrix. The predicted distribution matrix and the text domain distribution matrix are then utilized to compute matching loss.

features, bridging the gap between vision representation and the keypoint.

Domain Distribution Matrix Matching. To model cross-species keypoint-level relationships, we propose a domain distribution matrix that links keypoint categories to corresponding output heatmaps. Assuming we have 78 species and 15 keypoint categories per species, this leads to 1170 hypothetical (*animal species, keypoint category*) combinations. Directly representing each combination with a unique heatmap channel to model the above relationships is impractical. There exists cross-species commonality at the keypoint category level for OVKD since the keypoints of different animals may be similar. The similarity could be grasped during training by dividing all the keypoint categories into several groups and learning keypoint categories in the same group together. Therefore, we opt to represent multiple keypoint categories using a single channel of the ground-truth heatmaps. By grouping all keypoint categories and learning them collectively within these groups (where each group corresponds to one heatmap channel), we enhance the efficiency of the training process and avoid unnecessary computational expenditure. During testing, a new (*animal species, keypoint category*) combination is assigned to one of the predefined groups. The heatmap representation of the selected group is then utilized to detect keypoints for that specific combination. Consequently,

domain distribution matrix matching plays a crucial role in enhancing the prediction of new keypoint categories across various species.

Specifically, we apply K-means clustering to all training set keypoint categories, dividing them into O groups based on text embeddings generated by the Text_Encoder from $\{keypoint\ category\}$ terms. We then pre-compute a binary domain distribution matrix $\mathbf{D} \in \mathbb{R}^{K \times O}$ (setting $O = 100$) for each training sample, based on its keypoint categories. Here, K is a constant no smaller than any sample's maximum keypoint count. We set $\mathbf{D}_{ij} = 1$ when the i -th keypoint falls into the j -th group. If a sample's keypoint count K' is less than K , $\mathbf{D}_{ij} = 0$ for $i \in [K' + 1, K]$ and $j \in [1, O]$.

To learn group selection, we predict the distribution matrix. First, the updated visual features $\tilde{\mathbf{V}}$ are merged with the original features to strengthen visual representation. These features pass through the Vision_Head, identical to the baseline, to generate heatmaps $\mathbf{H}' \in \mathbb{R}^{O \times H \times W}$. The Vision_Adapter then adjusts the visual features \mathbf{V}' from these heatmaps, and the Keypoint_Adapter adjusts the text embeddings \mathbf{T}' from the original ones. Finally, we measure the similarity between the adjusted visual features $\mathbf{V}' \in \mathbb{R}^{C \times O}$ and the adjusted text embeddings $\mathbf{T}' \in \mathbb{R}^{K \times C}$ to create a predicted distribution matrix $\mathbf{P} \in \mathbb{R}^{K \times O}$:

$$\mathbf{P} = \mathbf{T}' \times \mathbf{V}'. \quad (6)$$

Loss Function. The matching loss L_{match} , computed as the cross-entropy loss between the predicted distribution matrix \mathbf{P} and the domain distribution matrix \mathbf{D} , aims to align keypoint categories with heatmap channels:

$$L_{match} = - \sum_{i=1}^K \sum_{j=1}^O \mathbf{D}_{ij} \log \mathbf{P}_{ij}. \quad (7)$$

Since the predicted heatmap ordering does not correspond to the prompt ordering, during testing, we need to determine the position j -th of the heatmap corresponding to the i -th prompt based on the predicted domain distribution matrix. Then, we reorder the heatmaps \mathbf{H}' generated by Vision_Head are reordered among channels according to the domain distribution matrix \mathbf{D} , which ensures that the heatmaps are aligned correctly with their corresponding prompts. For reordering, we locate the index o of the element 1 in the i^{th} row of \mathbf{D} , indicating that the o^{th} channel of \mathbf{H}' matches the i^{th} prompt. Functions like “`torch.index_select`” in Pytorch facilitate this reordering. The reordered heatmaps $\mathbf{H} \in \mathbb{R}^{O \times H \times W}$ are compared against ground truth heatmaps $\mathbf{G} \in \mathbb{R}^{O \times H \times W}$ using Mean Squared Error (MSE) loss. The first k channels of \mathbf{G} correspond to keypoint positions from the k text prompts, while the remaining channels are set as invalid zero matrices. The total loss function for training KDSM is:

$$L_{total} = \alpha L_{match} + \beta MSE(\mathbf{H}, \mathbf{G}), \quad (8)$$

where α and β are the balance weights, and they are set to $1e^{-6}$ and 1 unless otherwise specified. We follow (Xu et al., 2022a) to built \mathbf{G} , and the size of \mathbf{G} is the same as $\mathbf{H} \in \mathbb{R}^{O \times H \times W}$ ($O = 100, H = 64, W = 64$ in our implementation). Only the first k channels in \mathbf{G} are valid, corresponding to the k input prompts, with the rest set to zero.

Inference Process. During the inference phase, when presented with an input image and corresponding text prompts, KDSM replicates its training methodology to estimate the keypoint heatmaps and the predicted distribution matrix. This process involves a detailed analysis for each keypoint category k . Specifically, we search for the maximum value in the k -th row of the predicted distribution matrix, which identifies the index of the corresponding heatmap channel for that particular keypoint.

Once the indexes are determined, the heatmaps are carefully reordered and calibrated to align with these indexes, thus serving as the final prediction results. This step is crucial in ensuring the accuracy of our keypoint localization. Subsequently, the keypoint localization is precisely decoded as the coordinates that correspond to the highest scores within these reordered heatmaps.

4 Experiments

4.1 Open-Vocabulary Evaluation Protocol

Dataset Split. MP-100 (Xu et al., 2022a) is introduced for category-agnostic pose estimation, which contains over 20K instances covering 100 sub-categories and 8 super-categories (human hand, human face, animal body, animal face, clothes, furniture, and vehicle). However, some of the keypoint categories in MP-100, such as those for clothes and furniture, lack practical semantic information and are not suitable for language-driven OVKD. Thus, we selected a subset of 78 animal categories (including human) with keypoint annotations that have specific, meaningful semantic information. We call this subset “MP-78”, including COCO (Lin et al., 2014), AFLW (Koestinger et al., 2011), OneHand10K (Wang et al., 2018), AP-10K (Yu et al., 2021), Desert Locust (Graving et al., 2019), MasquePose (Labuguen et al., 2021), Vinegar Fly (Pereira et al., 2019), AnimalWeb (Khan et al., 2020), CUB-200 (Welinder et al., 2010).

MP-78 encompasses more than 14,000 images accompanied by 15,000 annotations. The annotations for the two experimental settings within the MP-78 dataset will be made publicly available alongside our source code. For keypoint types possessing semantic meaning, albeit lacking a precise definition or description, we employ ChatGPT to query and acquire the names of these keypoints. For example, we use a query like “How to anatomically describe the second joint of the index finger?” to obtain the name of a specific keypoint. All these queries are performed manually, and then we build the dataset MP-78.

It is essential to clarify that in this paper, $\{animal\ species\}$ refers to a combination of “target keypoint detection task + animal species.” For instance, the face and body of a dog are categorized as two distinct $\{animal\ species\}$ entities (i.e., “dog face” and “dog body”), based on the specific keypoint detection task. This means that our definition of species extends beyond mere biological classification, encapsulating task-specific categories within each animal.

To evaluate the generalization ability of OVKD to different keypoint categories and animal species, we design two settings, that is “Setting A: Diverse Keypoint Categories” for new $\{keypoint\ category\}$, and “Setting B: Varied Animal Species” for new $\{animal\ species\}$ like (Xu et al., 2022a). All zero-shot settings strictly fall under “transductive generalized zero-shot learning (Pourpanah et al., 2022)”.

In Setting A, we divide the keypoint categories associated with each of the 78 species into two parts: seen $\{keypoint\ category\}$ and unseen $\{keypoint\ category\}$. During training, we only used the seen categories, while the unseen categories were reserved for testing. For fair evaluation, we randomly split seen $\{keypoint\ category\}$ for each

Table 1: Comparisons with the baseline framework on the MP-78 dataset for Setting A. KDSM significantly outperforms the baseline.

Framework	Split1	Split2	Split3	Split4	Split5	Mean(PCK)
Baseline	42.02	44.00	42.55	43.80	42.26	42.93
KDSM	87.93	88.50	87.64	88.28	88.82	88.23

Table 2: Comparisons on MP-78 dataset for Setting B. KDSM notably demonstrates comparable performance on par with other few-shot species class-agnostic keypoint detection approaches.

Framework	Shot setting	Split1	Split2	Split3	Split4	Split5	Mean(PCK)
MAML (Finn et al., 2017)	5-shot	76.37	75.53	71.15	69.46	67.55	72.01
Fine-tune (Nakamura and Harada, 2019)	5-shot	77.81	76.51	72.55	71.09	69.85	73.56
FS-ULUS (Lu and Koniusz, 2022)	5-shot	78.34	79.67	76.89	81.52	75.23	78.33
POMNet (Xu et al., 2022a)	5-shot	81.25	86.44	81.01	86.93	78.68	82.86
CapeFormer (Shi et al., 2023)	5-shot	91.01	90.95	87.90	91.90	87.23	89.80
MAML (Finn et al., 2017)	1-shot	75.11	74.31	69.80	68.22	67.44	70.98
Fine-tune (Nakamura and Harada, 2019)	1-shot	76.65	76.41	71.37	69.97	69.36	72.75
FS-ULUS (Lu and Koniusz, 2022)	1-shot	73.69	70.65	63.97	71.14	63.65	68.62
POMNet (Xu et al., 2022a)	1-shot	73.07	77.89	71.79	78.76	70.26	74.35
CapeFormer (Shi et al., 2023)	1-shot	85.41	88.39	83.53	85.74	80.04	84.62
Baseline	zero-shot	56.06	55.36	54.35	53.07	50.66	53.90
KDSM	zero-shot	85.48	89.45	84.29	86.25	81.17	85.33

Table 3: Impact of hyperparameter settings on the performance of KDSM in Setting A for the OVKD task.

α	β	Split1	Split2	Split3	Split4	Split5	Mean(PCK)
1	1	13.57	13.22	13.26	12.80	13.78	13.32
1×10^{-1}	1	42.87	31.06	32.34	14.16	31.32	30.35
1×10^{-3}	1	79.02	71.35	76.68	79.79	74.67	76.30
1×10^{-4}	1	83.99	79.96	87.50	87.32	85.86	84.93
1×10^{-6}	1	87.93	88.50	87.64	88.28	88.82	88.23
1×10^{-7}	1	87.71	89.47	87.33	86.40	89.02	87.99
1×10^{-8}	1	30.50	30.02	30.54	30.36	28.77	30.04
1×10^{-10}	1	29.28	31.38	30.61	31.48	29.69	30.49
0	1	30.02	30.63	32.64	31.31	32.17	31.35

species to form seen {keypoint category} sets. We form five different train/test sets splits.

In Setting B, MP-78 is split into train/test sets, with 66 {animal species} for training, and 12 {animal species} for testing. To ensure the generalization ability of the framework, we evaluate the framework performance on five splits like (Xu et al., 2022a), where each {animal species} is treated as a novel one on different splits to avoid {animal species} bias.

Evaluation Metrics. We adopt the Probability of Correct Keypoint (PCK) to measure keypoint detection accuracy. This involves assessing the accuracy of a predicted keypoint by comparing its normalized distance from the actual ground-truth location, concerning a predefined threshold (σ). Consistent with the methodologies of POMNet (Xu et al., 2022a) and CapeFormer (Shi et al., 2023), we present the mean PCK@0.2 results in our experiments, setting σ at 0.2, for every category within each dataset split. In addition, to minimize category bias, we calculate and report the average PCK across all dataset splits, ensuring a balanced and comprehensive evaluation of our model’s keypoint detection performance.

4.2 Implementation Details

In our setup, the default Vision_Encoder is ResNet50 (He et al., 2016), pre-trained on the ImageNet dataset by default unless otherwise specified. The Self_Attn. module consists of three layers, each featuring a multi-head self-attention mechanism and a feed-forward neural network (FFN). This self-attention component is equipped with four attention heads and an embedding dimension of 512, with a dropout rate set at 0.1. The FFN includes two fully connected layers, an embedding dimension of 512, and 2048 feedforward channels. We employ ReLU as the activation function and maintain a dropout rate of 0.1. The Cross_Attn. component also comprises three layers. Each layer incorporates a multi-head self-attention mechanism, a multi-head cross-attention mechanism, and an FFN. The FFN configuration mirrors that of the Self_Attn. For text encoding, we default to using CLIP (Radford et al., 2021)’s Text_Encoder, pre-trained alongside the ViT-B/32 Vision_Encoder on image-text paired data, unless an alternative specification is provided.

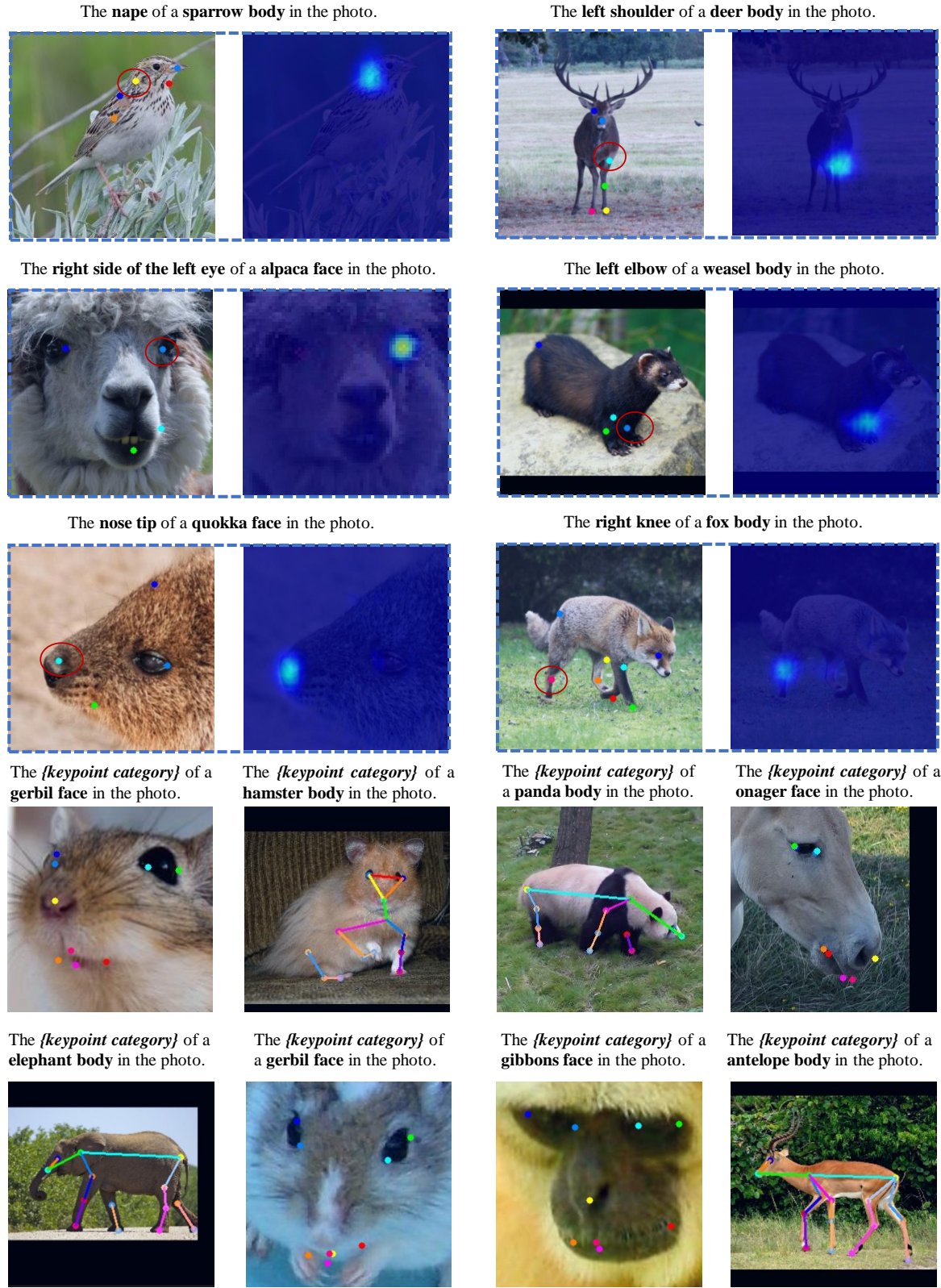


Fig. 4: Visual results of KDSM on the test sets of two experiment settings of OVKD. The first three rows show the heatmaps for Setting A, and the last two rows show the results for Setting B. KDSM achieves satisfactory results in both two settings. Due to space limitations, we use $\{\text{keypoint category}\}$ to represent the keypoint categories.

Table 4: Ablation study of proposed components on MP-78 for OVKD. Setting A is selected as the experiment setting.

Baseline	DDMM	VKLA	Split1	Split2	Split3	Split4	Split5	Mean(PCK)
✓	✗	✗	42.02	44.00	42.55	43.80	42.26	42.93
✓	✓	✗	69.64	57.86	67.95	62.10	71.92	65.89
✓	✓	✓	79.02	71.35	76.68	79.79	74.67	76.30

Table 5: Performance comparison of different attention blocks in Setting A for the OVKD task.

Self_Attention	Cross_Attention	Split1	Split2	Split3	Split4	Split5	Mean(PCK)
1	3	65.43	53.78	48.80	56.90	57.97	56.58
2	3	74.89	61.87	69.55	78.56	70.39	71.05
3	3	79.02	71.35	76.68	79.79	74.67	76.30
4	3	82.49	83.15	72.00	76.66	74.33	77.73
3	1	77.04	71.16	65.19	69.18	66.65	69.84
3	2	79.44	69.07	78.38	76.49	73.75	74.43
3	4	79.62	67.00	75.69	76.41	71.71	74.09

Table 6: Performance comparison of Text_Encoder with different Vision_Encoder configurations in Setting A for the OVKD task. CLIP represents that we replace the ResNet50 image encoder with the pre-trained ViT-B/32 image encoder of CLIP (Radford et al., 2021).

Text_Encoder	Vision_Encoder	Split1	Split2	Split3	Split4	Split5	Mean(PCK)
Paired with ResNet50	ResNet50	60.60	50.34	65.61	60.07	40.89	55.50
Paired with ViT-B/32	ResNet50	79.02	71.35	76.68	79.79	74.67	76.30
Paired with ViT-B/16	ResNet50	82.39	72.58	73.69	80.89	81.82	78.27
Paired with ViT-B/32	ViT-B/32 (CLIP)	52.54	49.25	59.23	50.30	45.17	51.30

The objects of interest are extracted using their bounding boxes and resized to dimensions of 256×256 . To bolster the model’s generalization capabilities, data augmentation techniques such as random scaling (varying from -15% to 15%) and random rotation (varying from -15° to 15°) are applied. Training is carried out across 4 GPUs, each with a batch size of 64, for a total of 210 epochs. The Adam optimizer (Kingma and Ba, 2014) is employed, starting with an initial learning rate of $1e^{-3}$. This learning rate is subsequently decreased to $1e^{-4}$ at the 170th epoch and to $1e^{-5}$ at the 200th epoch.

4.3 Results for OVKD

Setting A: Diverse Keypoint Categories. Table 1 presents the performance comparison between the baseline framework and KDSM on the MP-78 dataset for this setting. The table highlights that KDSM consistently surpasses the baseline in all five dataset splits. The quantitative comparison of the results shows a significant performance improvement when using the KDSM framework. The Mean(PCK) score across all five splits increases from 42.93% for the baseline to 88.23% for the KDSM framework, which corresponds to a 45.30 percentage point enhancement. This indicates that the KDSM approach is more effective at handling the “Diverse Keypoint Categories” setting in the zero-shot fashion. The superior performance of the KDSM framework on the “Diverse Keypoint Categories” setting can be attributed to its capacity to better

align and match semantic information from text prompts with local visual features, as well as its ability to effectively transfer knowledge to unseen (*animal species, keypoint category*) pairs.

Setting B: Varied Animal Species. Table 2¹ displays the performance comparison between the baseline framework and KDSM on the MP-78 dataset for the “Varied Animal Species” setting under a zero-shot setting. Additionally, it compares the results with class-agnostic keypoint detection methods under 1-shot and 5-shot settings.

The KDSM framework significantly outperforms the baseline in the zero-shot setting, demonstrating its effectiveness in handling unseen animal species without category-specific training. The enhanced performance of the KDSM framework is due to the efficient knowledge transfer from seen to unseen $\{\text{animal species}\}$. Besides, recent research (Shi et al., 2023; Xu et al., 2022a) has developed few-shot species class-agnostic keypoint detection techniques that can identify keypoints across various animal species without category-specific training. However, these techniques typically rely on support images with annotations during both the training and testing phases. In contrast, our OVKD approach using the KDSM framework does not require support images by leveraging text prompts $\{\text{animal species}\}$ and $\{\text{keypoint category}\}$ for semantic guidance.

¹ We refer to the method “Few-shot keypoint detection with uncertainty learning for unseen species” as FS-ULUS.

Table 7: Performance of KDSM on different super-categories in Setting A for the OVKD task.

Super-Category	Split1	Split2	Split3	Split4	Split5	Mean(PCK)
Face	85.05	77.56	83.52	87.31	76.01	81.89
Body	76.73	68.61	73.67	76.37	74.49	73.97
Face w/ Body	79.02	71.35	76.68	79.79	74.67	76.30

OVKD and few-shot species class-agnostic keypoint detection represent distinct methodological approaches, making direct comparisons challenging, so we primarily benchmark against our baseline. However, we also highlight the performance gap contrast with few-shot species class-agnostic keypoint detection methods at a macro level. Our method shows results comparable to these few-shot species class-agnostic keypoint detection approaches, and excels against the state-of-the-art CapeFormer (Shi et al., 2023)’s 1-shot solution, underscoring the efficacy of our method. Moreover, our zero-shot OVKD even outperforms 5-shot setting of FS-ULUS (Lu and Koniusz, 2022), MAML (Finn et al., 2017), Fine-tune (Nakamura and Harada, 2019), and POMNet (Xu et al., 2022a). Notably, methods like POMNet and CapeFormer are limited during training as they cannot access images of new categories but rely on support images during testing. Thus, it’s reasonable for our zero-shot method to exhibit better performance than 1-shot solutions.

4.4 Ablation Study

In this section, we do some ablation experiments about the hyperparameter settings of the loss function, domain distribution matrix matching, vision-keypoint relational awareness module, Vision_Encoder and Text_Encoder. The default setting is $\alpha = 1e^{-3}$ and $\beta = 1$.

Discussion of the Loss Function of KDSM. We explore various hyperparameter configurations in this section. Table 3 illustrates how these settings impact KDSM’s performance in the OVKD Setting A evaluation. We observe that as the value of α is reduced from 1 to 10^{-10} , while maintaining β at a constant 1, the Mean(PCK) shows an increasing trend. The optimal performance is attained at $\alpha = 10^{-6}$, resulting in a Mean(PCK) of 88.23. Conversely, further reducing α below 10^{-6} , or setting it to 0, leads to a decrease in Mean(PCK), suggesting an ideal range for α ’s value. Notably, when α is set to 0, the Mean(PCK) falls sharply to 31.15, underscoring the significance of domain distribution matrix matching.

Domain Distribution Matrix Matching. Table 4 reveals that Domain Distribution Matrix Matching (DDMM) notably enhances Mean(PCK) scores, boosting them from 42.93% to 65.89%. This substantial increase attests to DDMM’s effectiveness in promoting knowledge transfer between seen and unseen keypoint categories. Moreover, the uniform improvement across all dataset splits underscores the robustness

and adaptability of our proposed method, emphasizing its suitability for diverse real-world applications.

Vision-Keypoint relational Awareness Module. Table 4 shows that integrating the baseline framework with both Domain Distribution Matrix Matching and Vision-Keypoint Relational Awareness Module leads to a notable increase in Mean(PCK) scores. Precisely, the Mean(PCK) score escalates from 42.93% in the baseline without these components to 76.30% when incorporating both DDMM and VKLA modules. This improvement underscores the critical necessity of the VKLA module in our methodology, as it adeptly discerns the semantic connections between visual features and text prompts, thereby enhancing generalization capabilities for unseen keypoint categories.

Attention Layers in Vision-Keypoint relational Awareness Module. Our study also delves into the optimal number of self-attention and cross-attention layers within the VKLA module. The findings, as depicted in Table 5, indicate that augmenting the number of self-attention blocks from 1 to 3 leads to a marked improvement in performance (compare row 1 with row 3). However, adding a fourth self-attention block doesn’t contribute substantially to further gains (compare row 3 with row 4). A similar pattern is observed with the number of cross-attention blocks, leading us to implement three cross-attention blocks in our final configuration.

Discussion on the Choice of Vision Encoder. Following previous research (Ni et al., 2022), we train a task-specific visual encoder instead of fine-tuning the original CLIP visual encoder, but we both still leverage the language model’s knowledge (that is why we can achieve OVKD). As shown in Table 6, the ResNet50-based visual encoder outperforms the CLIP pre-trained ViT-B/32 model. This is because OVKD involves handling diverse pose variations and joint localization, which requires dense region-level features, while the CLIP visual encoder learns the global image-level features.

Discussion on the Choice of Text Encoder. Table 6 presents a comparison of using Text_Encoders, each pre-trained with different Vision_Encoders, for the OVKD task. The Mean(PCK) scores are as follows: 55.50 for ResNet50, 76.30 for ViT-B/32, and 78.27 for ViT-B/16, with the Text_Encoder corresponding to ViT-B/16 Vision_Encoder exhibiting the highest performance. This variation in performance among the Text_Encoders implies that employing a more robust Text_Encoder, specifically one that is pre-trained with a more powerful Vision_Encoder, leads to improved results. While we used ViT-B/32 in this paper, this finding



Fig. 5: Visual results of challenging KDSM on the test sets of two experiment settings of OVKD. (a) Demonstrates that KDSM can handle challenging scenarios involving body occlusion, environmental occlusion, and complex poses. (b) Illustrates the failure cases of KDSM in challenging keypoint detection. The points circled in red represent the ground truth keypoint locations corresponding to the heatmaps. The blue circles enclose the challenging regions of keypoint detection. Due to space limitations, we use *{keypoint category}* to represent the keypoint categories.

suggests significant potential for enhancing our method’s performance by integrating a stronger Text_Encoder.

Discussion of OVKD Task for Different Super-Categories. To assess KDSM’s capability in managing various super-categories within the OVKD task, we segregated the MP-78 dataset into two distinct, non-overlapping super-categories: Face and Body. Table 7 demonstrates KDSM’s differing performance in these categories. Specifically, it achieved Mean(PCK) scores of 81.89 for the Face category and 73.97 for the Body category, clearly showing a superior performance in the Face category. The comparatively lower score for the Body category likely stems from the more complex and varied body poses. Despite the strong results, there appears to be potential for further enhancement, particularly in the Body category’s performance.

4.5 Qualitative Results

In Fig. 4, we display KDSM’s outcomes under two experimental settings of OVKD. The first three rows illustrate the heatmaps for new keypoint categories, while the last two rows present the actual keypoint detection results. These visual representations clearly demonstrate KDSM’s proficiency in successfully accomplishing the OVKD task across both settings.

4.6 Future work

Our research focuses on achieving OVKD, a new and promising research topic, with satisfactory performance on regular scenes. Further improvement in challenging scenarios (e.g., occlusion, lighting, and resolution) will be left for our future

work. Unlike traditional methods that rely on manual annotation, OVKD offers valuable recognition to arbitrary keypoints without prior annotation. Furthermore, we include some results of our method’s performance in occlusion scenarios in Fig. 5(a), demonstrating its capability to handle certain occlusion cases effectively. However, we also present some instances where our method encounters challenges under occlusion, as seen in Fig. 5(b), indicating areas for potential improvement.

5 Conclusion

We address the challenges inherent in traditional image-based keypoint detection methods for animal (including human) body and facial keypoint detection by introducing the **Open-Vocabulary Keypoint Detection** (OVKD) task. This task is designed to identify keypoints in images, regardless of whether the specific animal species and keypoint category have been encountered during training. Our novel framework, **Open-Vocabulary Keypoint Detection with Semantic-feature Matching** (KDSM), leverages the synergy of advanced language models to effectively bridge the gap between text and visual keypoint features. KDSM integrates innovative strategies such as **Domain Distribution Matrix Matching** (DDMM) and other special modules, such as the **Vision-Keypoint Relational Awareness** (VKRA) module, leading to significant performance enhancements. Specifically, we observed a 45.30-point improvement in detecting diverse keypoint categories and a 31.43-point improvement for varied animal species compared to the baseline framework. Notably, KDSM achieves comparable results with those of state-of-the-art few-shot species class-agnostic keypoint detection methods. The proposed approach lays the groundwork for future exploration and advancements in OVKD, driving further improvements in quantitative performance metrics.

Declarations

Data Availability The dataset MP-100 for this study can be downloaded at: <https://github.com/luminxu/Pose-for-Everything>. Our reorganized and partitioned dataset MP-78 will be released together with our source code.

Conflict of interest The authors declare that they have no conflict of interest.

References

Hanoona Bangalath, Muhammad Maaz, Muhammad Uzair Khattak, Salman H Khan, and Fahad Shahbaz Khan. Bridging the gap between object and image-level representations for open-vocabulary detection. *Advances in Neural Information Processing Systems*, 35: 33781–33794, 2022.

Tom Brown, Benjamin Mann, Nick Ryder, Melanie Subbiah, Jared D Kaplan, Prafulla Dhariwal, Arvind Neelakantan, Pranav Shyam, Girish Sastry, Amanda Askell, et al. Language models are few-shot learners. *Advances in neural information processing systems*, 33: 1877–1901, 2020.

Nicolas Carion, Francisco Massa, Gabriel Synnaeve, Nicolas Usunier, Alexander Kirillov, and Sergey Zagoruyko. End-to-end object detection with transformers. In *Computer Vision–ECCV 2020: 16th European Conference, Glasgow, UK, August 23–28, 2020, Proceedings, Part I 16*, pages 213–229. Springer, 2020.

Alexey Dosovitskiy, Lucas Beyer, Alexander Kolesnikov, Dirk Weissenborn, Xiaohua Zhai, Thomas Unterthiner, Mostafa Dehghani, Matthias Minderer, Georg Heigold, Sylvain Gelly, et al. An image is worth 16x16 words: Transformers for image recognition at scale. *arXiv preprint arXiv:2010.11929*, 2020.

Chelsea Finn, Pieter Abbeel, and Sergey Levine. Model-agnostic meta-learning for fast adaptation of deep networks. In *International conference on machine learning*, pages 1126–1135. PMLR, 2017.

Jacob M Graving, Daniel Chae, Hemal Naik, Liang Li, Benjamin Koger, Blair R Costelloe, and Iain D Couzin. Deepposekit, a software toolkit for fast and robust animal pose estimation using deep learning. *Elife*, 8:e47994, 2019.

Kaiming He, Xiangyu Zhang, Shaoqing Ren, and Jian Sun. Deep residual learning for image recognition. In *Proceedings of the IEEE conference on computer vision and pattern recognition*, pages 770–778, 2016.

Chao Jia, Yinfai Yang, Ye Xia, Yi-Ting Chen, Zarana Parekh, Hieu Pham, Quoc Le, Yun-Hsuan Sung, Zhen Li, and Tom Duerig. Scaling up visual and vision-language representation learning with noisy text supervision. In *International Conference on Machine Learning*, pages 4904–4916. PMLR, 2021.

Muhammad Haris Khan, John McDonagh, Salman Khan, Muhammad Shahabuddin, Aditya Arora, Fahad Shahbaz Khan, Ling Shao, and Georgios Tzimiropoulos. Animalweb: A large-scale hierarchical dataset of annotated animal faces. In *Proceedings of the IEEE/CVF Conference on Computer Vision and Pattern Recognition*, pages 6939–6948, 2020.

Diederik P Kingma and Jimmy Ba. Adam: A method for stochastic optimization. *arXiv preprint arXiv:1412.6980*, 2014.

Martin Koestinger, Paul Wohlhart, Peter M Roth, and Horst Bischof. Annotated facial landmarks in the wild: A large-scale, real-world database for facial landmark localization. In *2011 IEEE international conference on computer vision workshops (ICCV workshops)*, pages 2144–2151. IEEE, 2011.

Rollyn Labuguen, Jumpei Matsumoto, Salvador Blanco Negrete, Hiroshi Nishimaru, Hisao Nishijo, Masahiko Takada, Yasuhiro Go, Kenichi Inoue, and Tomohiro Shibata. Macaquepose: a novel “in the wild” macaque monkey pose dataset for markerless motion capture. *Frontiers in behavioral neuroscience*, 14:581154, 2021.

Boyi Li, Kilian Q Weinberger, Serge Belongie, Vladlen Koltun, and René Ranftl. Language-driven semantic segmentation. *arXiv preprint arXiv:2201.03546*, 2022.

Tsung-Yi Lin, Michael Maire, Serge Belongie, James Hays, Pietro Perona, Deva Ramanan, Piotr Dollár, and C Lawrence Zitnick. Microsoft coco: Common objects in context. In *Computer Vision–ECCV 2014: 13th European Conference, Zurich, Switzerland, September 6–12, 2014, Proceedings, Part V 13*, pages 740–755. Springer, 2014.

Changsheng Lu and Piotr Koniusz. Few-shot keypoint detection with uncertainty learning for unseen species. In *Proceedings of the IEEE/CVF Conference on Computer Vision and Pattern Recognition*, pages 19416–19426, 2022.

Akihiro Nakamura and Tatsuya Harada. Revisiting fine-tuning for few-shot learning. *arXiv preprint arXiv:1910.00216*, 2019.

Bolin Ni, Houwen Peng, Minghao Chen, Songyang Zhang, Gaofeng Meng, Jianlong Fu, Shimeng Xiang, and Haibin Ling. Expanding language-image pretrained models for general video recognition.

In *Computer Vision–ECCV 2022: 17th European Conference, Tel Aviv, Israel, October 23–27, 2022, Proceedings, Part IV*, pages 1–18. Springer, 2022.

Yingwei Pan, Ting Yao, Yehao Li, and Tao Mei. X-linear attention networks for image captioning. In *Proceedings of the IEEE/CVF conference on computer vision and pattern recognition*, pages 10971–10980, 2020.

Talmo D Pereira, Diego E Aldarondo, Lindsay Willmore, Mikhail Kislin, Samuel S-H Wang, Mala Murthy, and Joshua W Shaevitz. Fast animal pose estimation using deep neural networks. *Nature methods*, 16(1):117–125, 2019.

Farhad Pourpanah, Moloud Abdar, Yuxuan Luo, Xinlei Zhou, Ran Wang, Chee Peng Lim, Xi-Zhao Wang, and QM Jonathan Wu. A review of generalized zero-shot learning methods. *IEEE transactions on pattern analysis and machine intelligence*, 2022.

Rui Qian, Yeqing Li, Zheng Xu, Ming-Hsuan Yang, Serge Belongie, and Yin Cui. Multimodal open-vocabulary video classification via pre-trained vision and language models. *arXiv preprint arXiv:2207.07646*, 2022.

Alec Radford, Jong Wook Kim, Chris Hallacy, Aditya Ramesh, Gabriel Goh, Sandhini Agarwal, Girish Sastry, Amanda Askell, Pamela Mishkin, Jack Clark, et al. Learning transferable visual models from natural language supervision. In *International conference on machine learning*, pages 8748–8763. PMLR, 2021.

Min Shi, Zihao Huang, Xianzheng Ma, Xiaowei Hu, and Zhiguo Cao. Matching is not enough: A two-stage framework for category-agnostic pose estimation. In *IEEE/CVF Conference on Computer Vision and Pattern Recognition, CVPR 2023, Vancouver, BC, Canada, June 17–24, 2023*, pages 7308–7317. IEEE, 2023.

Jun Tu, Gangshan Wu, and Limin Wang. Dual graph networks for pose estimation in crowded scenes. *International Journal of Computer Vision*, pages 1–21, 2023.

Ashish Vaswani, Noam Shazeer, Niki Parmar, Jakob Uszkoreit, Llion Jones, Aidan N Gomez, Łukasz Kaiser, and Illia Polosukhin. Attention is all you need. *Advances in neural information processing systems*, 30, 2017.

Jingdong Wang, Ke Sun, Tianheng Cheng, Borui Jiang, Chaorui Deng, Yang Zhao, Dong Liu, Yadong Mu, Mingkui Tan, Xinggang Wang, et al. Deep high-resolution representation learning for visual recognition. *IEEE transactions on pattern analysis and machine intelligence*, 43(10):3349–3364, 2020.

Yangang Wang, Cong Peng, and Yebin Liu. Mask-pose cascaded cnn for 2d hand pose estimation from single color image. *IEEE Transactions on Circuits and Systems for Video Technology*, 29(11):3258–3268, 2018.

Peter Welinder, Steve Branson, Takeshi Mita, Catherine Wah, Florian Schroff, Serge Belongie, and Pietro Perona. Caltech-ucsd birds 200. 2010.

Tingyu Weng, Jun Xiao, Hao Pan, and Haiyong Jiang. Partcom: Part composition learning for 3d open-set recognition. *International Journal of Computer Vision*, pages 1–24, 2023.

Bin Xiao, Haiping Wu, and Yichen Wei. Simple baselines for human pose estimation and tracking. In *Proceedings of the European conference on computer vision (ECCV)*, pages 466–481, 2018.

Lumin Xu, Sheng Jin, Wang Zeng, Wentao Liu, Chen Qian, Wanli Ouyang, Ping Luo, and Xiaogang Wang. Pose for everything: Towards category-agnostic pose estimation. In *Computer Vision–ECCV 2022: 17th European Conference, Tel Aviv, Israel, October 23–27, 2022, Proceedings, Part VI*, pages 398–416. Springer, 2022a.

Mengde Xu, Zheng Zhang, Fangyun Wei, Han Hu, and Xiang Bai. Side adapter network for open-vocabulary semantic segmentation. In *Proceedings of the IEEE/CVF Conference on Computer Vision and Pattern Recognition*, pages 2945–2954, 2023.

Yufei Xu, Jing Zhang, Qiming Zhang, and Dacheng Tao. Vitpose+: Vision transformer foundation model for generic body pose estimation. *arXiv preprint arXiv:2212.04246*, 2022b.

Lewei Yao, Jianhua Han, Youpeng Wen, Xiaodan Liang, Dan Xu, Wei Zhang, Zhenguo Li, Chunjing Xu, and Hang Xu. Detclip: Dictionary-enriched visual-concept paralleled pre-training for open-world detection. *arXiv preprint arXiv:2209.09407*, 2022.

Hang Yu, Yufei Xu, Jing Zhang, Wei Zhao, Ziyu Guan, and Dacheng Tao. Ap-10k: A benchmark for animal pose estimation in the wild. *arXiv preprint arXiv:2108.12617*, 2021.

Hao Zhang, Shenqi Lai, Yaxiong Wang, Zongyang Da, Yujie Dun, and Xueming Qian. Segnet: Shifting and cascaded group network. *IEEE Transactions on Circuits and Systems for Video Technology*, 2023.

Xiayang Zhu, Renrui Zhang, Bowei He, Ziyu Guo, Ziyao Zeng, Zipeng Qin, Shanghang Zhang, and Peng Gao. Pointclip v2: Prompting clip and gpt for powerful 3d open-world learning. In *Proceedings of the IEEE/CVF International Conference on Computer Vision*, pages 2639–2650, 2023.